A Methodology for Autonomous Radio Repeating Based on the A* Algorithm

Bryan Krawiec* and Kevin Kochersberger†

Unmanned Systems Lab, Virginia Tech, Blacksburg, VA, 24060, USA

David C. Conner‡

TORC Robotics, Blacksburg, VA, 24060, USA

In the event of a disaster, first responders must rapidly gain situational awareness about the environment in order to plan effective response operations. Unmanned ground vehicles are well suited for this task but often require a strong communication link to a remote ground station to effectively relay information. When considering an obstacle-rich environment, non-line-of-sight conditions and naïve navigation strategies can cause substantial degradations in radio link quality. Therefore, this paper incorporates an unmanned aerial vehicle as a radio repeating node and presents a path planning strategy to cooperatively navigate the vehicle team so that radio link health is maintained. This navigation technique is formulated as an A*-based search and this paper presents the formulation of this path planner as well as an investigation into strategies that provide computational efficiency to the search process. The path planner uses predictions of radio signal health at different vehicle configurations to effectively navigate the vehicles and simulations have shown that the path planner produces favorable results in comparison to several conceivable naïve radio repeating variants. The results also show that the radio repeating path planner has outperformed the naïve variants in both simulated environments and in field testing where a Yamaha RMAX unmanned helicopter and a ground vehicle were used as the vehicle team.

Nomenclature

ϵ	Heuristic inflation factor
f	Total cost
F_{Sum}	Fresnel ellipsoid intersection sum
g	Cost term
g_{FEC}	Fresnel ellipsoid cost
g_{GVDC}	Ground vehicle distance cost
g_{RLBC}	Radio link budget cost
g_{RLDC}	Radio link difference cost
$G_{t/r}$	Power gain term for transmitter/receiver antenna
h	Heuristic term
h_{HLUT}	Heuristic look-up table
$L_{Cable_{t/r}}$	Cable power loss at transmitting/receiving radio
$L_{Conn_{t/r}}$	Connector power loss at transmitting/receiving radio
L_{Path}	Path loss term for radio link
P_r	Radio received signal strength
P_t	Radio transmitted power
X	State Space

*Graduate Research Assistant, Department of Mechanical Engineering, Virginia Tech

†Associate Professor, Department of Mechanical Engineering, Virginia Tech

‡Adjunct Assistant Professor, Bradley Department of Electrical and Computer Engineering, Virginia Tech

$\mathbf{x}$	State vector
(x_G, y_G)	Ground vehicle position coordinates
(x_H, y_H)	Helicopter position coordinates
x_{max}	state space x coordinate boundary
y_{max}	state space y coordinate boundary
V	Four-dimensional discretized grid of resolution Δv_i in each coordinate

I. Introduction

In the event of a disaster in a populated area, whether it is of natural, accidental, or deliberate origin, first responders need to quickly evaluate the post-disaster environment in order to assess damages and plan effective response operations. Unfortunately, post-disaster environments typically pose a number of dangers to the responders. These dangers may consist of collapsed buildings that block planned ingress or egress routes, structures that may be on the verge of collapsing, or harmful particulates in the air that may be hazardous to the health of the responders. Without the proper situational awareness about the presence of these dangers, response operations would be ill-informed and the lives of both civilians and the responders themselves may be put at risk. On the other hand, unmanned ground vehicles (UGVs) provide the distinct advantages that they do not suffer from the same health limitations as humans and they are relatively expendable when put in comparison to a human life. These characteristics, combined with the fact that these vehicles can be equipped with a variety of sensing and communication equipment, make them ideal candidates for performing initial investigations of the potentially dangerous post-disaster environments. By performing these initial investigations, when first responders execute response operations and enter the post-disaster environment themselves, they will have a more well-informed concept of their surroundings thereby leading to safer and more efficient response efforts.

Despite these benefits, unmanned ground vehicles still suffer from the major flaw that they typically require communication with a ground control station in order to effectively accomplish a mission. Since many missions involving UGVs are carried out in complex environments where buildings, obstacles, or hills in the terrain exist between the ground station and the UGV, the UGV will likely enter non-line-of-sight scenarios with the ground station. This can cause substantial degradations in the radio communication link which can result in data packet errors or even a loss of the communication link entirely.

In order to resolve this communication limitation, the Unmanned Systems Lab (USL) proposes adding an unmanned aerial vehicle (UAV) to the operation as a radio repeating node in the communication link. By employing this concept, communications can be relayed from the ground station, through the aerial vehicle, and to the ground vehicle. This allows the aerial vehicle to act as an antenna in the sky, which can increase the effective communication range of the ground vehicle to regions beyond-line-of-sight from the ground station. Even with this concept though, a naïve choice for the position of the aerial vehicle could still result in a number of non-line-of-sight scenarios between the vehicles which can provide similarly degraded communication links. Therefore, this work formulates this radio repeating operation as an A*-based path planning problem where the vehicles are cooperatively navigated so that the UGV can approach a target location while maintaining a strong radio repeating link with the ground station.

The remainder of this paper is organized as follows. Section II provides background and relevant related work from the literature. Section III then formulates the path planning problem as an A*-based search process and provides simulation results that assess the path planner's performance. Section IV continues by discussing the incorporation of this path planner on a Yamaha RMAX unmanned helicopter and a ground vehicle and the results of field testing that was performed. Finally, Section V summarizes the details presented in this paper and offers insight into the most relevant contributions of this work.

II. Background

The development of a system capable of performing a radio repeating operation involves a number of aspects ranging from research into the concept of radio repeating for a robotic system to the formulation of the path planning strategy itself. This section therefore presents background information and prior work that is related to these aspects. Several prior efforts in communication-aware robotic operations are first discussed to provide perspective on this subject and then a brief discussion on relevant details for A*-based path planning is given.

A. Communication-Aware Robotic Operations

Communication-aware strategies for the navigation of unmanned vehicles are becoming more prevalent in the literature as researchers attempt to deploy them in more complicated mission scenarios. These developments, at least in the field of multi-robot operations, have been recent and as Hsieh and Kumar discuss in a 2004 paper,[1] much of the literature on multi-robot operations up to that date focused on areas like control and planning, while naïvely assuming that the robots can freely communicate with each other regardless of their configuration. Based on the literature considered in the development of the work presented here, the communication-aware path planning strategies seem to focus on two types of operations. The first involves using similar radio repeating concepts for enhancing communication networks and the other involves using unmanned vehicles for mapping radio signal strengths throughout an environment.

Examples of using radio repeating concepts in the recent literature are relatively numerous. For example, one paper[2] discusses the benefit of using a UAV as a communications relay for warfighters and the importance of using a dynamically changing communications system. This concept is employed by Dixon and Frew,[3,4] for example, who present work on radio leashing where they have developed controllers for a fixed wing UAV so that it maintains either constant signal-to-noise ratio orbits from radio sources or follows a gradient path to the best signal-to-noise ratio location. Separately, a series of papers[5–8] use a group of slave ground robots as repeater nodes for a lead ground robot that investigates an indoor environment. In this work, the slave robots are deployed as a bread crumb trail, per se, to enhance the radio link between a remote operator and the lead robot. While these papers serve as inspiration for the radio repeating work, they all tend to be corrective and act according to radio measurements taken during an operation. The work presented here differs in that the vehicles are navigated in a more predictive manner based on a path planner that considers predicted gains and losses associated with the radio link components. In this way, although the presented path planner may be somewhat open-loop in nature, the vehicles have a more well-informed general concept of how to navigate themselves to maintain favorable radio performance than they would otherwise.

In contrast with this, the other primary set of papers reviewed involve mapping radio signal strengths throughout an environment. For example, Hsieh, Kumar, and Taylor[1] discuss a method of formulating an exploration problem in order to create a radio signal strength map that can be used in subsequent planning operations. This work was also extended[9] to be implemented with a multi-robot team. In this work, each robot was assigned a list of waypoints and measurements of radio signal strengths were taken between the pairs of robots. These measurements then formed a radio connectivity map that the authors envision being used to plan paths for the multi-robot team in other operations. Also, in a recent 2010 publication, the GRASP lab extended its work[10] to use this radio mapping concept along with Gaussian processes to localize a radio signal source in an environment. Additionally, Ayad, Nielson, and Voyles[11] discuss very preliminary work to perform radio mapping with robots and to understand the relationship between sources of interference and changes in radio signal strengths. While it is true that generating radio maps would be beneficial for a planning operation and could add corrective behavior to the planner presented below if radio maps could be constructed online, many times in response operations time is of the essence and it is impractical to waste precious time generating these radio maps. Therefore, the work of this thesis seeks to perform communication-aware path planning without necessarily having a complete radio map of the area.

B. A*-Based Path Planning

With the motivation of formulating the radio repeating operation as a path planning problem, a particular path planning algorithm had to be chosen. Even though numerous path planning techniques exist in the literature,[12] Ferguson[13] notes that while the two most popular distinctions for planning come in the form of heuristic-based algorithms and randomized algorithms, when the dimension of the planning problem is low, the heuristic-based approaches are usually preferred due to their ability to provide optimality or suboptimality guarantees on the resulting paths. Considering the radio repeating scenario in this work, it is treated as a relatively low dimensional path planning problem and since there is great interest to optimize the quality of the path with respect to the performance of the radio links between the vehicles, the heuristic-based methods were chosen for this work. More specifically, the A* algorithm was chosen specifically due to its optimality guarantees.[14,15]

Expanding on this, the A* algorithm is considered to be a general graph search method from a start state to a goal state where transitions between the states are quantified by a cost function.[14] This cost function, denoted as f, consists of an accrued cost term g that penalizes state transitions for undesirable behavior and a heuristic h that guides the search towards the goal state. Throughout the path planning process, this algorithm seeks to minimize the cost function as it progresses from the start to the goal and as long as the heuristic is both consistent and admissible,[14] the resulting paths are guaranteed to be optimal. This allows the A* algorithm great versatility since the cost function can be customized to fit a specific path planning scenario.

While this algorithm in its basic form provides a systematic means of generating optimal paths, it can be relatively computationally intensive when applied to large or high-dimensional state spaces. Therefore, in addition to its widespread popularity, this concern has sparked a significant amount of research into different modifications and enhancements to the algorithm to provide it with more efficiency. For example, Hansen and Zhou[14] discuss an inflated heuristic variant of the A* algorithm, known as the Weighted A* (WA*) algorithm, where the heuristic for the search is inflated to provide enhanced computational efficiency at the expense of optimality. For this search, the cost function f is instead formulated with an inflation factor ϵ on the heuristic where $\epsilon > 1$.

$$f = g + \epsilon h \tag{1}$$

Although the true optimality of the resulting paths are sacrificed in this WA* search, the resulting paths are guaranteed to be ϵ-suboptimal for a heuristic that is inflated by a factor of ϵ where the resulting paths are at worst ϵ times the cost of the optimal path.[13] Also, as Hansen and Zhou[14] point out, this method is well suited for planning problems where a number of close-to-optimal paths exist since the WA* algorithm can find these close-to-optimal paths in only a tiny fraction of the time that it takes to generate an optimal path.

A series of simulations have shown that the WA* search can produce close-to-optimal paths in a fraction of the time that it takes the A* search to generate optimal paths. Table 1 for example displays averaged results from two-dimensional searches through 50 random obstacle-rich maps. For these simulations, the start position for the search was the upper left corner of the map and the goal was the lower right corner. Additionally, the cost function used for the searches was the distance traveled from the start and the heuristic was the straight line Euclidean distance to the goal. As is shown in the table, even small ϵ inflation factors result in substantially improved computational efficiencies which can be noted by the amount of closed and open states considered in the searches. While the distinction between these types of states is important to the mechanics of the WA* algorithm, for comparative purposes, it suffices to say that the closed states are those that a search has considered completely and has determined the least cost paths for, whereas the open states are those that have been encountered but not evaluated completely. Due to the expansive nature of this search algorithm, the open states are generally at the boundaries of the search. Figure 1 displays example paths and the amounts of open and closed states for a set of two-dimensional searches where the closed states are represented as green pixels, the open states as blue pixels, and the obstacles as red pixels. Additionally, when considering the path costs, even the highly inflated $\epsilon = 100$ searches generated paths that were on average only 3.7 percent higher in cost than the optimal path cost. This provides confidence that this inflated heuristic search can be employed rapidly and with reasonable suboptimal results.

Table 1. 2D Weighted A* simulation data averaged over 50 random environments

Epsilon	Closed States	Open States	Path Cost	Fraction Optimal Closed States	Fraction Optimal Path Cost
100.0	454	1344	523.341	0.014	1.037
20.0	457	1343	523.202	0.014	1.036
10.0	464	1343	523.023	0.014	1.036
5.0	476	1345	521.110	0.014	1.032
1.5	604	1359	510.589	0.019	1.011
1.2	1462	1395	506.484	0.045	1.003
1.0	32726	2346	504.872	1.000	1.000

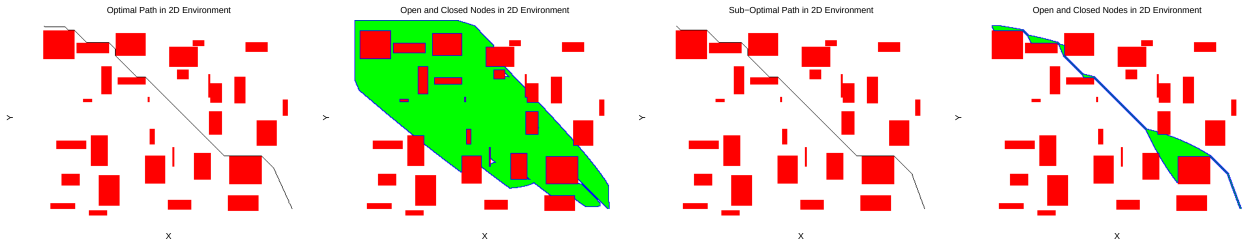

(a) Optimal path ($\epsilon = 1$) (b) Open/closed ($\epsilon = 1$) (c) Suboptimal path ($\epsilon = 1.2$) (d) Open/closed ($\epsilon = 1.2$)

Figure 1. Examples of an WA* paths and open/closed states for different ϵ inflation factors using a straight line Euclidean distance heuristic that is well-informed

While the above results provide very convincing evidence for the benefit of using the WA* search, the algorithm generated such powerful results because the heuristic used in the search was well-informed. That is, since the paths were evaluated based on a g cost that measured distance traveled, a heuristic that was also based on a distance measure could very effectively guide the searches. In order to assess whether the same computational benefits could be seen with an ill-informed heuristic, another batch of simulations was performed. These simulations were formulated in the same manner as the prior ones but also incorporated a random 1 to 64 valued cost at each state transition to mimic uncertainty in the search environment that was not taken into account by the heuristic. This extra cost term could intuitively result from uncertainties in the terrain due to sensing deficiencies or from obstacles in the terrain map not taken into consideration by the heuristic. The addition of this cost term makes the heuristic ill-informed since the straight line Euclidean distance heuristic is no longer well correlated with the g cost terms that quantify the performance of the search. With the addition of this cost and due to the fact that its magnitude makes it the dominant term in the cost function, the heuristic cannot guide the search as effectively as in the prior simulations. As noted in Table 2, small inflation factors such as $\epsilon = 1.2$ no longer provide the computational benefits as when employed with a well-informed heuristic. However, using higher inflation factors like $\epsilon = 20$ provides substantially reduced computational efforts while still generating near optimal paths. When considering that the theoretical bound for the path cost of an $\epsilon = 20$ search is 20 times the optimal path cost, the fact that an average result was produced that was only 1.174 times that of the optimal path cost is quite remarkable. Also, figure 2 shows example results from the simulations with the random costs added to the environments.

Table 2. 2D Weighted A* simulation data averaged over 50 random environments with random terrain costs

Epsilon	Closed States	Open States	Path Cost	Fraction Optimal Closed States	Fraction Optimal Path Cost
100.0	474	1416	12181.830	0.005	1.849
20.0	1703	1850	7738.606	0.018	1.174
10.0	70459	4416	6653.174	0.725	1.010
5.0	95063	4543	6595.405	0.978	1.001
1.5	97180	4411	6590.121	1.000	1.000
1.2	97199	4410	6590.121	1.000	1.000
1.0	97211	4409	6590.121	1.000	1.000

Two key points can be noted from the ill-informed heuristic simulations. The first is that searches at high inflation factors can still produce near optimal results with only a small fraction of the computational effort as searches without an inflated heuristic. The second is that it would be beneficial to have a well-informed heuristic to effectively guide the search if possible. This is especially so in more complex higher-dimensional searches and this motivates the use of a heuristic look-up table which is visually depicted in figure 3. Basically, rather than using a straight line Euclidean distance heuristic in an obstacle-rich environment, a more well-informed heuristic can be generated by performing an initial two-dimensional search through the environment and using its results as a heuristic for higher dimensional searches.[13] By considering figure

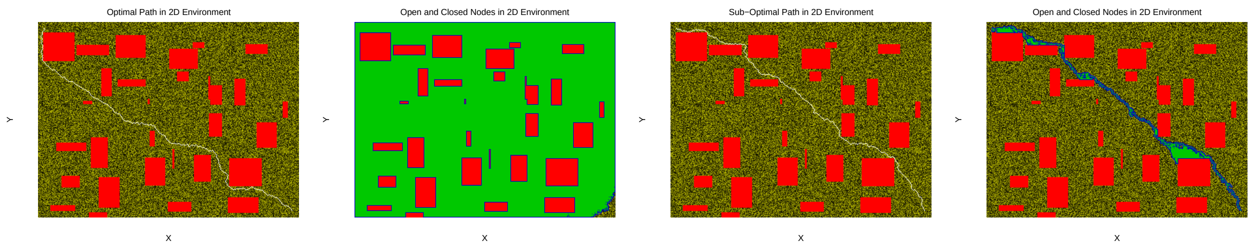

(a) Optimal path ($\epsilon = 1$) (b) Open/closed ($\epsilon = 1$) (c) Suboptimal path ($\epsilon = 20$) (d) Open/closed ($\epsilon = 20$)

Figure 2. Examples of an WA* paths and open/closed states for different ϵ inflation factors using a straight line Euclidean distance heuristic that is ill-informed

3 where the red colors indicate higher heuristic values and the blue indicate lower ones, it is obvious that the heuristic look-up table more effectively guides the search. In fact, when considering the radio repeating path planner discussed in the next section, using the Euclidean distance heuristic resulted in 145996 total states considered in the search whereas using the heuristic look-up table resulted in only 3378 total states considered in the search. By incorporating this heuristic look-up table concept with a highly inflated WA* search, large computational benefits can be gained that make the A*-based methods suitable for the more complex radio repeating path planning discussed below.

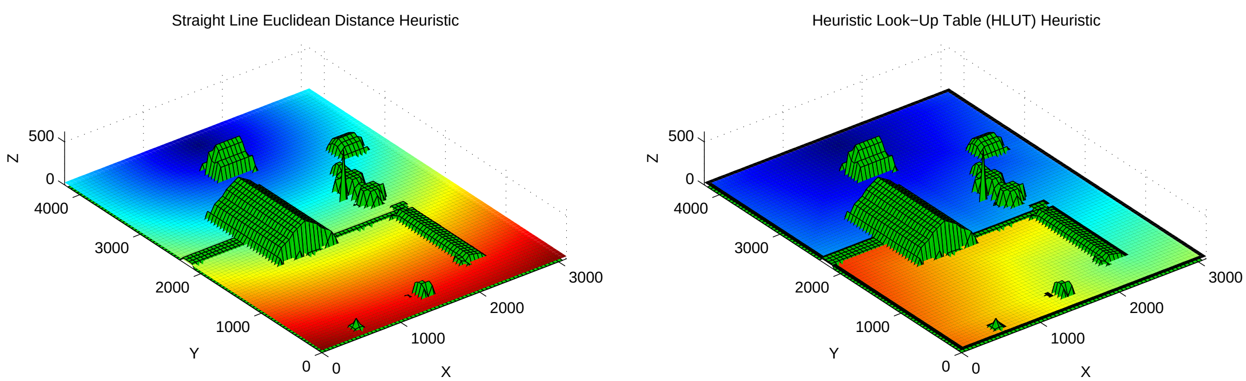

(a) Euclidean distance (b) HLUT

Figure 3. Visual display of heuristic values for straight line Euclidean distance and heuristic look-up table (HLUT) heuristics with red indicating large and blue indicating small values

III. A* Radio Repeating Path Planner

As noted above, the WA* algorithm is a very versatile path planning technique that can be catered to a particular scenario of interest. For this work, it is a radio repeating scenario where an unmanned helicopter is employed as a radio repeating node to extend the range of a ground vehicle from a fixed ground station. The planner is therefore formulated so that near-optimal paths are generated which guide the ground vehicle to a desired goal location while a strong radio repeating link to the ground station is maintained. For this planner, the resulting paths are waypoint trails for the ground vehicle and helicopter which could easily be tracked in such a way that as the ground vehicle approaches a particular waypoint, the helicopter is guided to its corresponding one. For the purposes of this work, the ground vehicle is intended to be unmanned but as will be shown in Section IV, the resulting unmanned system can easily be extended to the case of a manned vehicle. Also, due to the computational benefits of the WA* algorithm, this path planning process can be executed rapidly and requires only knowledge of the positions of the vehicles, a goal location for the ground vehicle, and a terrain map of the environment to operate properly. Therefore, this planner can be executed online during a mission operation. To provide clarity on the formulation and performance of the planner, this section details the selection of the state space and cost function for the path planner as well as practical considerations that were taken into account when developing each. Then, this section continues to present simulated testing results for the path planner and comparisons to simulated results from other naïve radio repeating variants to show its ability to outperform several simplified radio repeating methods.

A. Radio Repeating Path Planner Formulation

In order to effectively formulate the radio repeating path planner as a WA* variant, the state space and the cost function for the search require definition. Starting by considering the state space, a few realizations can be made. First, in the radio repeating scenario there are two radio links that need to be maintained in order for the communication link to be healthy. The first is the link between the ground station and the unmanned helicopter and the second is the link between the helicopter and the ground vehicle. Since the quality of these links are dependent upon the positions of both vehicles, the navigation of the vehicles, and correspondingly the state space for the path planner, is coupled. Therefore, the state space must contain states for both vehicles.

Second, when considering a general aerial vehicle control problem, there are typically 12 states associated with the vehicle. These correspond to the positions, velocities, angular attitudes, and angular velocities of the aerial vehicle. Similarly, a ground vehicle can be modeled with 5 states consisting of its position in a plane, its forward velocity, its yaw angle, and its yaw rate. If all of these states were taken into account though, the planning problem would be 17-dimensional which would be unwieldy for rapid implementation.

Fortunately, many unmanned helicopters, inclusive of the Yamaha RMAX used in this work, are equipped with stabilizing control systems that allow them to maintain a hover state while accepting velocity commands to guide them to a particular waypoint. A similar claim can be made for ground vehicles. Therefore, rather than dealing with all 17 states, the path planning can be simply performed on the 3 positions associated with the helicopter (x,y,z) and the two positions associated with the ground vehicle (x,y). This drastically reduces the computational complexity of the path planner and allows it to be amenable to rapid execution.

Furthermore, due mainly to practical considerations, the z state of the helicopter position is also eliminated making the state space 4-dimensional in nature. This is primarily for safety reasons in that it is much safer to set the helicopter to a fixed altitude throughout a testing operation, however, an extension of the work presented here could be to incorporate the z helicopter state which could be helpful in very complex urban environments where heights of buildings are less uniform than those tested here. Therefore, the state vector for the path planner is as follows.

$$\mathbf{x} = \begin{bmatrix} x_G \\ y_G \\ x_H \\ y_H \end{bmatrix} \tag{2}$$

Since the A* path planning method is a discrete search technique, the state space is represented as a 4-dimensional grid and for practical considerations, the grid is bounded by a region where a terrain map of the environment is known. Written mathematically, this state space can be expressed as

$$X = \{\mathbf{x} \in V | \mathbf{0} \leq \mathbf{x} \leq [x_{max}, y_{max}, x_{max}, y_{max}]^T\}$$

where the inequality is component-wise, x_{max} and y_{max} are the upper boundaries of the terrain map, and V represents a discretized grid of resolution Δv_i in each of the four dimensions. For clarification, figure 4 depicts the state space for the radio repeating scenario. It should be noted that in order to properly assess the costs of the cost function developed next, an approximate terrain map of an environment is required for the path planner. For the Unmanned Systems Lab, this is not an unreasonable assumption since work is also performed in the area of using stereovision techniques to reconstruct 3D terrain models of an environment[16] and recent developments have shown promising results.

Considering the cost function for the radio repeating scenario, it has been crafted to guide a ground vehicle to a goal location while penalizing navigation that is not indicative of maintaining healthy radio links. Each term in the cost function is included to provide specific performance and by compiling the various costs together, the radio repeating path planner provides desirable performance. The various costs are given as follows.

1. Ground vehicle distance cost

2. Radio link budget cost
3. Radio link difference cost
4. Fresnel ellipsoid cost

Starting with the ground vehicle distance cost, this cost accumulates the distance that is traveled by the ground vehicle throughout the search. This cost is included since providing the ground vehicle with a relatively short path to a goal location is a desired performance characteristic and it is expressed mathematically below. Here the summation is performed over the n points along the paths considered by the planner.

$$g_{GVDC} = \sum_{i=1}^{n} \|\mathbf{x}_i - \mathbf{x}_{i-1}\|_2 \tag{3}$$

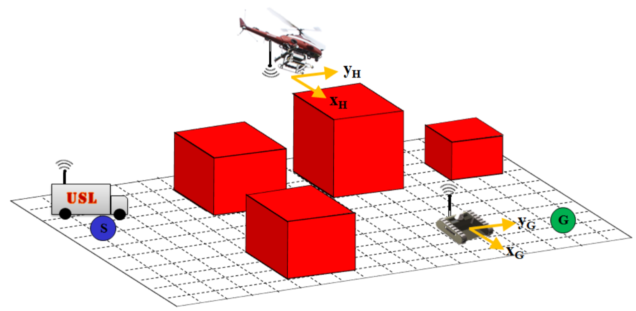

Figure 4. Diagram for radio repeating state space

Next, the radio link budget cost was implemented to predict and quantify the strengths of the radio repeating links throughout the search. This cost uses predicted received signal strengths of the radio links as metrics and this cost accrues at each state transition based on the vehicle configurations throughout the search. The choice of using the received signal strength of a radio link as a metric was based on the observation[10] that the received signal strength of a radio link has been heavily correlated to the bit error rate of a communication link and therefore the health of the radio link as well. Using the Friis Transmission Equation,[17] converting it to a decibel scale, and abstracting the path losses to a single term, a link budget for the radio link can be given as follows.

$$P_r = P_t - L_{Conn_t} - L_{Cable_t} + G_t - L_{Path} + G_r - L_{Conn_r} - L_{Cable_r} \tag{4}$$

Here, the received signal strength (P_r) is based on the transmitted power (P_t), losses in the cables and connectors ($L_{Cable_{t/r}}$,$L_{Conn_{t/r}}$), gains from the antennas ($G_{t/r}$), and propagation losses incurred in the transmission path from the transmitting antenna to the receiving antenna (L_{Path}). When considering these terms, the transmitted power is generally set and is a value of $P_t = 30$ dBm for the 1 W radios used, the cable and connector losses are reasonably accurately determined from data sheets which are 2.3 dB in total, and the antenna gains have been determined experimentally. Figure 5 displays the vertical cross section of the antenna pattern for the omnidirectional antennas used by the Unmanned Systems Lab and it should be noted that the pattern is symmetric with respect to the horizontal plane. With these known quantities, the only term that requires characterization is the path loss term L_{Path} which accounts for all of the losses both from the $\frac{1}{R^2}$ free space propagation and effects from the multipath propagation associated with an obstacle-rich environment.

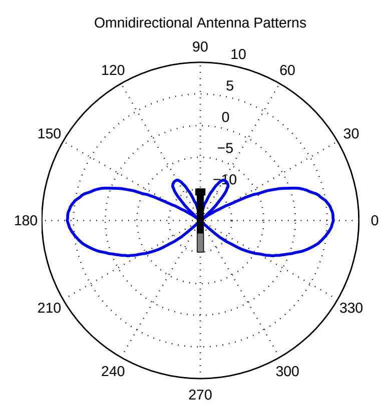

Figure 5. Polar plot of gains associated with the vertical cross section of an omnidirectional antenna radiation pattern

Based on the literature considered, two major methodologies exist for determining these path losses. The first methodology is to model the path losses based on deterministic calculations. As noted by Neskovic et al.[18] though, the accurate prediction of radio signal strengths is often a very complex task requiring extensive databases of an environment's propagation characteristics which are typically overly time consuming to obtain. Coupling this complexity with the facts that the propagation environment in a disaster response situation is poorly known to the required accuracy of deterministic methods and that the path planning calculations need to possibly be calculated thousands of times in a very short time frame makes these deterministic methods infeasible for path planning situations. A more simplified approach though is to use empirical methods.[18] These methods use models that are based on extensive path loss measurements in different propagation environments. Because of this, all of the complicating factors involved with the deterministic calculations are implicitly taken into account. While Neskovic et al.[18] note that the accuracy of these models is surely based on the similarities between the environment of interest and where the measurements were taken, they serve as computationally simple tools for estimating path losses. One of the earliest and most widely cited papers on empirical models was written by Hata[19] who presents empirical models based on Okumura's[20] extensive path loss data for a variety of propagation environments in Japan. Additionally, other models such as the one created by Walfisch and Bertoni[21] and those referenced by other empirical model studies[22,23] are also common. In order to determine the most appropriate model to use with the radio repeating path planner, path loss testing was performed in the farm environment where the USL is permitted to fly its unmanned aerial vehicles. While this environment is open, it is hilly and contains a number of buildings that can block the line-of-sight between the transmitting and receiving antennas. Path loss testing results are shown in figure 6 and statistical residual analyses have shown that the Hata Open model is most appropriate for predicting line-of-sight path losses whereas the Hata Suburban model is most appropriate at predicting non-line-of-sight path losses at the particular environment tested. This is of course exclusive of very short path lengths where the roll-off of the Hata Open model is too severe and the free space losses are recommended to be used instead as a conservative estimate of path losses.

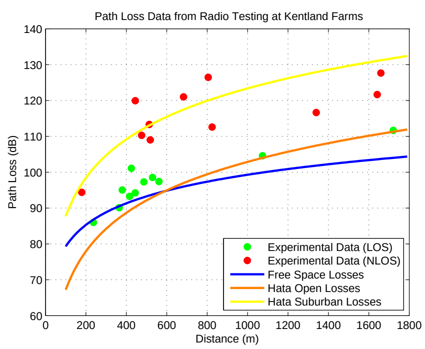

Figure 6. Path loss data from radio testing at USL flight test site

By incorporating these empirical models with the radio link budget, received signal strengths can be predicted for different vehicle configurations. These signal strengths are incorporated into the cost term below and this cost attempts to maximize the received signal strengths of the repeating links throughout the search process.

$$g_{RLBC} = \sum_{i=1}^{n} \|\mathbf{P}_{Received,i}\|_2 \tag{5}$$

$$\mathbf{P}_{Received,i} = \begin{bmatrix} (P_t - P_r)_{GroundStation-to-Heli,i} \\ (P_t - P_r)_{Heli-to-GroundVehicle,i} \end{bmatrix} \tag{6}$$

Additionally, due to the logarithmic nature of the empirical path loss models, some simulations have shown the potential for one link to get biased over the other. Therefore, in order to maintain the health of both links throughout the search process, another cost term has been added to penalize differences in the links' received signal strengths. This is expressed mathematically as follows.

$$g_{RLDC} = \sum_{i=1}^{n} |(P_t - P_r)_{GroundStation-to-Heli,i} - (P_t - P_r)_{Heli-to-GroundVehicle,i}| \tag{7}$$

Lastly, when considering the effects of the above costs, they serve to guide the ground vehicle toward a goal location and maintain the predicted signal strengths of the radio links. However, due to the substantial increase in path losses associated with the non-line-of-sight test data of figure 6, the path planner could be improved further by incorporating a cost that penalizes not only intersections between obstacles and the line-of-sight path between the transmitter and receiver but also between obstacles and the first Fresnel ellipsoid[24] of the transmitter and receiver pairs. By keeping these regions free of obstacles, line-of-sight conditions can be observed and the deleterious effects of multipath propagation can be minimized. Therefore, the final cost term in the cost function is as follows.

$$g_{FEC} = 100 \sum_{i=1}^{n} \left(F_{Sum,GroundStation-to-Heli,i} + F_{Sum,Heli-to-GroundVehicle,i}\right) \tag{8}$$

Here the F terms are terms that accrue based on the amount of penetration of obstacles from the environment into the first Fresnel ellipsoids of the radio links. In order to accomplish this, the ellipsoids for the first Fresnel zones are calculated, they are translated and rotated to their appropriate locations for each vehicle configuration, a number of points on the ellipsoids are sampled, and intersections are checked between those points and obstacles in the environment. It should be noted that a terrain model of the environment of interest is critical for the calculation of this term. This term, however, allows the vehicles to maintain line-of-sight wherever possible in a particular environment and vastly improves the signal strengths of the radio links. Lastly, it should be noted that the 100 factor for this cost was chosen to make it one of the most dominant terms in the cost function and was selected in an ad hoc manner by performing a number of simulations.

Combining these costs with a heuristic look-up table that provides a well-informed heuristic and also penalizes obstacle and environment boundary intersections, the total cost function for the radio repeating path planner can be written as follows.

$$f = g_{GVDC} + g_{RLBC} + g_{RLDC} + g_{FEC} + \epsilon h_{HLUT} \tag{9}$$

B. Radio Repeating Path Planner Simulations

In order to test the performance of the radio repeating path planner, it was coded in the MATLAB environment and a number of randomized simulations were performed with the intent of determining an objective an unbiased assessment of the planner's abilities. In each set of simulations, 10 random start and goal locations were chosen for the ground vehicle where the start positions were placed on one side of the environment and the goal positions on the opposite side. This restriction was chosen to maintain consistency between the simulations and so that the ground vehicle would always have to traverse through the bulk of the map in its planning. Additionally, also to maintain consistency between simulations, the aerial vehicle's start position was always placed immediately adjacent to the ground vehicle and the ground station was always at a fixed point towards one corner of the environment. An example starting configuration for the system is shown in figure 7.

By inspecting this figure, it may be intuitive that different arrangements of obstacles may result in different performances from the path planner. As one might expect, the more clutter there is in the environment, the less likely the planner may be able to maintain line-of-sight conditions and the planner's performance may suffer accordingly. Therefore, in addition to simply testing different start and goal locations for the same environment, a variety of environments were tested. More specifically, fifteen environments were tested in total with the environments segregated into three distinct categories. These environment types were arbitrarily named Type I, II, and III environments where Type I environments mimicked open environments with relatively sparse arrangements of obstacles, Type II environments mimicked campus environments with orderly and more dense arrangements of obstacles, and Type III environments mimicked even more dense suburban environments. Examples of these map types are shown in figure 8. Coupling the fact that fifteen environments were tested (5 for each type) with the fact that 10 start/goal combinations were simulated for each map, 150 simulations were performed in total to assess the performance of the radio repeating path planner.

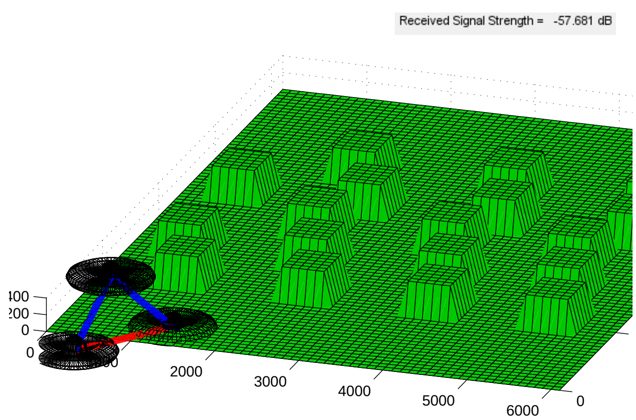

Figure 7. Example of starting configuration for radio repeating simulations

In addition to this, since it would not be too enlightening to test the path planner without a baseline for comparison, four other naïve radio repeating variants were also formulated and tested under the same conditions as the radio repeating path planner. These variants, which were generated by the authors, incorporate two-dimensional searches that use the ground vehicle distance cost to navigate the ground vehicle to its goal location, but take more simplified approaches to navigating the helicopter. These serve as a useful group to compare the radio repeating path planner's performance with since they represent fairly intuitive but naïve ways to perform the radio repeating operation. Since they do not consider the costs associated with the radio link health that have been used in the radio repeating path planner, they are less sophisticated than the planner and therefore provide useful baselines for assessing the planner's performance. These variants are described as follows.

1. **Naïve 1**– The helicopter is positioned at a single location at the center of the environment.
2. **Naïve 2**– The helicopter is strictly positioned above the goal location for the ground vehicle.

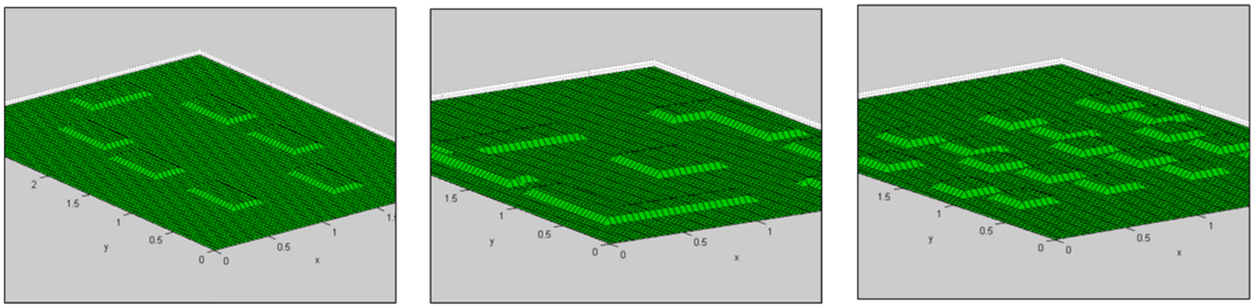

(a) Type I (b) Type II (c) Type III

Figure 8. Example maps for radio repeating simulation environment types

3. **Naïve 3**– The helicopter is maintained exactly over the ground vehicle as it traverses from the start to the goal locations.

4. **Naïve 4**– The helicopter is positioned strictly at the midpoint of the ground vehicle's path from the start to the goal.

The results of simulations for each map type are shown in Table 3 and the overall results averaged over all map types are shown in Table 4. In these tables, the path planner and naïve variants are assessed not only on their computation times, but also on the average predicted signal strengths associated with the radio repeating links throughout the simulated navigation of the vehicles along their waypoint paths and the amount of non-line-of-sight incurred throughout this navigation as well. For example, the "Avg RSS GS-to-Heli" value represents the average of the received signal strengths for the ground station to helicopter radio link over a simulated navigation through a particular map with a particular start/goal combination. Therefore, the numbers displayed under "Map Type I Average Results", for example, are those values averaged over all of the Type I simulations. Similar results are provided for the received signal strengths of the helicopter to ground vehicle radio links and the amount of non-line-of-sight incurred throughout the simulations. The settings used for these simulations were a four dimensional state space of size 27,772,900, an inflation factor of $\epsilon = 10000$, a radio frequency of 2.4 GHz, a transmit power of 30 dBm, and a helicopter height of 20 m.

By inspecting these tables and based on the simulations performed, the radio repeating path planner generates desirable results and also outperforms the naïve variants. Although the computation time for the radio repeating path planner is greater than those of the naïve variants due to the fact that it is a 4-dimensional search as opposed to the 2-dimensional searches of the naïve variants, this is vastly overshadowed by the increases in both predicted radio link quality and in the amount of line-of-sight that the path planner was able to maintain. In Table 4, for example, the average received signal strength for the ground station to helicopter radio link was at least 9 dB higher than the those of the naïve counterparts on average. Also, the path planner was able to achieve at least 28 percent more line-of-sight behavior than the naïve variants for the ground station to helicopter link on average. Additionally, when considering the helicopter to ground vehicle link, the planner produced comparable results to the naïve variants and exhibited more line-of-sight behavior than all of the variants except the third naïve variant. However, the third naïve variant positions the helicopter strictly over the ground vehicle, which tends to produce very poor antenna gains and an overall poor performance anyway. Therefore, these results show that the path planner generally outperforms all of the naïve variants and therefore exhibits a navigation strategy that is more well-informed than those of the more simplified naïve variants. This provides confidence that in operation, the radio repeating path planner can guide the vehicles to configurations that will have a higher likelihood of producing stronger communication links than simplified alternatives where the health of the radio link is not actively taken into consideration.

In addition to this, even though the path planner outperforms the naïve variants on average, under the appropriate choices of start/goal positions, the planner can produce substantially better results than the naïve counterparts for the same start/goal combination. This is shown in Table 5 as the best case performance and as seen by the data in the table, the path planner produces very desirable results both in terms of average predicted received signal strengths throughout the vehicle navigation and in terms of amount

Table 3. Average radio repeating path planner and naïve radio repeating variant simulation results separated by map type

Simulation	Plan	Naïve I	Naïve II	Naïve III	Naïve IV
Start/Goal Sets per Map	10	10	10	10	10
Number of Maps per Type	5	5	5	5	5
Overall Average Simulation Results					
Closed States	80	80	80	80	80
Open States	3847	195	195	195	195
Computation Time	6.59	0.87	0.87	0.80	0.87
Map Type I Average Results					
Avg RSS GS-to-Heli	-53.7	-68.8	-74.7	-62.1	-64.7
% NLOS GS-to-Heli	5	60	58	28	42
Avg RSS Heli-to-GV	-53.6	-50.2	-58.0	-66.3	-51.1
% NLOS Heli-to-GV	12	11	28	0	16
Map Type II Average Results					
Avg RSS GS-to-Heli	-53.2	-64.3	-79.3	-64.0	-63.9
% NLOS GS-to-Heli	5	40	76	36	38
Avg RSS Heli-to-GV	-57.5	-57.9	-65.2	-66.3	-56.6
% NLOS Heli-to-GV	34	60	57	0	30
Map Type III Average Results					
Avg RSS GS-to-Heli	-53.9	-68.8	-83.4	-64.5	-66.0
% NLOS GS-to-Heli	9	60	92	39	48
Avg RSS Heli-to-GV	-53.3	-55.1	-62.1	-66.3	-53.9
% NLOS Heli-to-GV	17	40	42	0	29

Table 4. Radio repeating path planner and naïve radio repeating variant simulation results averaged over all map types

Simulation	Plan	Naïve I	Naïve II	Naïve III	Naïve IV
Number of Simulations	150	150	150	150	150
Average Results Over All Map Types					
Avg RSS GS-to-Heli	-53.6	-67.3	-79.1	-63.5	-64.9
% NLOS GS-to-Heli	6	53	75	34	43
Avg RSS Heli-to-GV	-54.8	-54.4	-61.8	-66.3	-53.9
% NLOS Heli-to-GV	21	37	42	0	25

Table 5. Best case radio repeating path planner simulation results as compared to naïve radio repeating variants

Simulation	Plan	Naïve I	Naïve II	Naïve III	Naïve IV
Map Type I Best Case Results					
Avg RSS GS-to-Heli	-48.9	-77.7	-59.4	-53.6	-54.1
% NLOS GS-to-Heli	0	100	0	0	0
Avg RSS Heli-to-GV	-51.2	-62.7	-67.8	-66.3	-50.1
% NLOS Heli-to-GV	1	74	71	0	10
Map Type II Best Case Results					
Avg RSS GS-to-Heli	-53.9	-55.4	-85.3	-59.5	-55.0
% NLOS GS-to-Heli	0	0	100	19	0
Avg RSS Heli-to-GV	-52.1	-58.8	-67.6	-66.3	-60.3
% NLOS Heli-to-GV	1	68	69	0	74
Map Type III Best Case Results					
Avg RSS GS-to-Heli	-51.8	-77.7	-85.3	-57.7	-54.9
% NLOS GS-to-Heli	0	100	100	11	0
Avg RSS Heli-to-GV	-50.7	-48.0	-58.2	-66.3	-53.4
% NLOS Heli-to-GV	1	0	23	0	26

of line-of-sight behavior exhibited. Therefore, based on the simulations performed, the radio repeating path planner produces desirable paths with respect guiding the ground vehicle to a goal location and maintaining strong radio repeating links in the process. Also, even though empirical models have been used to predict path losses which are only valid on average, the path planner's paths produce vehicle behaviors that, based on experience, are indicative of attempting to maintain healthy radio links.

IV. Vehicle System Testing

With the radio repeating path planner described above producing desirable results, the planner was implemented and tested on a vehicular system. This test provided two primary benefits for this work. The first was the validation that this planning operation could be performed on a complete system and be extended beyond just simulated results. The second was that the data taken from the test could partially validate the simulated results produced by the path planner. Specifically, the radio signal strengths measured throughout the flight test were compared with those predicted by the planner and also with those measured from a naïve radio repeating variant test. By doing this, not only could confidence be gained about the predicted signal strengths produced by the planner but also that the radio repeating path planner could produce better paths than a naïve counterpart from the standpoint of received signal strengths. Unfortunately though, due to the temporal and monetary constraints associated with flight tests, as well as the fact that regulations only permit the USL to fly its unmanned aircraft at one test facility, only one flight test could be performed. Therefore, even though the data presented in this chapter represents a small sample set, it provides confidence that the radio repeating path planner can perform as expected on a real vehicular system.

Figure 9 depicts the test setup for the radio repeating test. Figure 9(a) shows the Yamaha RMAX unmanned helicopter which was the UAV for the test. This helicopter includes a wePilot autopilot system that allows the helicopter to be operated fully autonomously and a Cobham COFDM radio that handles the data transmission throughout the test. Figure 9(b) shows the test facility that the radio repeating operation was performed at. As can be noted, there are several buildings in this test area that can generate non-line-of-sight scenarios for naïve vehicle operations and a terrain model of this area was constructed for the path planner to use in its planning. Lastly, figure 9(c) depicts the radio repeating test in operation.

This image shows the ground control station which contained a laptop and a Cobham radio that were used to handle the path planning and communication operations throughout the test, as well as a ground vehicle which contained another Cobham radio and a laptop to display path information to the driver of the vehicle. It should be noted that a manned ground vehicle was used to provide flexibility to the operation and that only minor changes would be required to perform the operation with an unmanned ground vehicle instead. Lastly, all of the code used in the planning, flight control, and communication operations was developed by the author in the NI LabVIEW and C++ coding languages. Therefore, in addition to just creating a path planner, this work involved all of the coding for a full-scale vehicle operation.

(a) Yamaha RMAX (b) Test Facility (c) Radio Repeating Operation

Figure 9. Images of various components in the radio repeating flight test

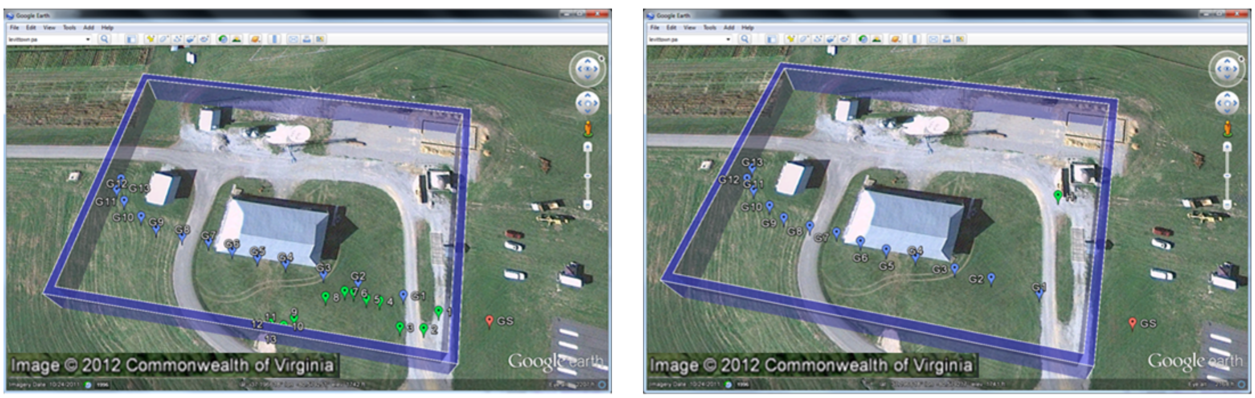

(a) Path Planner (b) Naïve Variant

Figure 10. Radio signal strength sample points for path planning and naïve radio repeating variants overlaid in Google Earth (© 2012 Google)

In this flight test, paths were planned for the ground vehicle and the helicopter, the ground vehicle was driven along its path, and as the ground vehicle approached each of its waypoints, the helicopter was autonomously flown to its corresponding waypoints. Figure 10(a) displays sample points from along the paths of the helicopter and ground vehicle where radio signal strength measurements were taken. In this figure, the green points represent the positions of the helicopter, the blue points represent the positions of the ground vehicle, the red point indicates the position of the ground station, and the blue boundary represents the borders of the environment used in the path planning. By inspecting the figure, performance indicative of maintaining strong radio repeating links is seen. As the ground vehicle drove to its destination in the left portion of the image, the helicopter swung out to enter the high gain portions of the antenna patterns, then it followed the ground vehicle while staying within those high gain regions, and as the ground vehicle traversed behind the final building, the helicopter swung outward to maintain line-of-sight with the ground station and the ground vehicle. Figure 10(b) on the other hand shows the same sample points but with the helicopter naïvely sitting at a stationary point in the environment.

Figure 11 shows the received signal strengths of the radio repeating links taken at the aforementioned sample points. From this data, the ground station to helicopter links are relatively similar between the two variants. This makes intuitive sense since, for this link, the helicopter is placed in similar configurations with

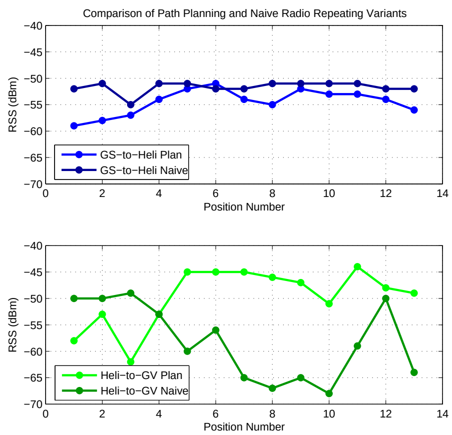

Figure 11. Comparison of received signal strengths for the radio repeating links sampled from the path planning and naïve radio repeating variant flight tests

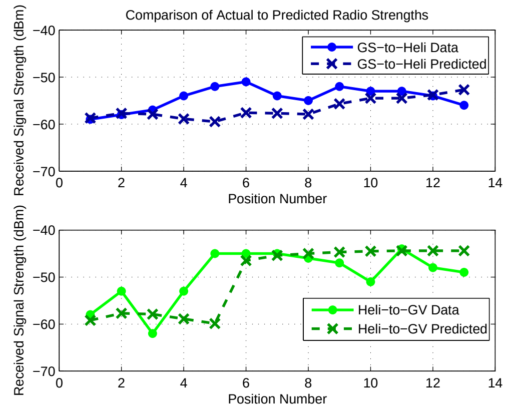

Figure 12. Comparison between predicted and actual radio signal strengths from the radio repeating path planner flight test

respect to distances, line-of-sight, and antenna gains for both variants. The helicopter to ground vehicle links though exhibit larger differences. In the path planning variant, barring the first few sample points where the helicopter is not quite in the high antenna gain regions, the received signal strengths were quite strong given the test setup. The naïve variant on the other hand exhibited very poor performance since it had no regard for the ground vehicle's distance, the antenna gains, or whether line-of-sight conditions existed or not.

Next, figure 12 provides plots of the predictions from the path planner for radio signal strengths as compared to those actually measured in the operation. As can be seen, the path planner's predictions match up well with the data in terms of thematic performance. Of course there are some discrepancies between the predictions and the data but these can be intuitively explained based on experimental complexities and on the fact that the empirical models are only average predictions. Some of these experimental complexities could have included potential offsets between the terrain model and the real world environment as well as the existence of small hills not specifically accounted for in the planner that could have caused the antennas mounted on the vehicles to rotate as the hills were traversed.

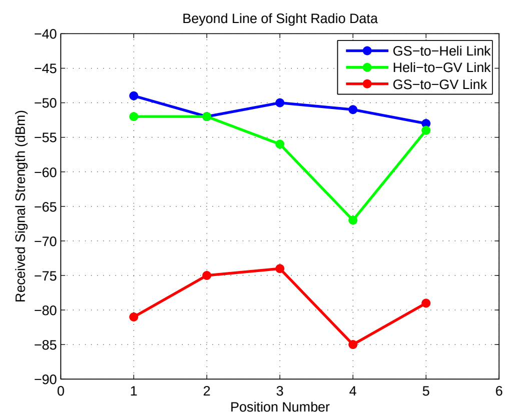

Figure 13. Comparison of radio repeating and ground link received signal strengths in beyond-line-of-sight ground vehicle testing

Lastly, in order to further validate the merit of the radio repeating concept and to emphasize its usefulness in beyond-line-of-sight ground vehicle operations, another set of data was collected where the ground vehicle was clearly in a non-line-of-sight scenario with the ground station. The data from this test is displayed in figure 13 and it shows that the radio repeating links produced respectable signal strengths while the ground station to ground vehicle link produced dangerously low signal strengths considering the distances tested. This data clearly shows the merit of the radio repeating concept in general while the test data of figure 11 clearly shows the merit of intelligently planning trajectories for the vehicles so that the strengths of the communication links are maintained.

V. Conclusion

Overall, this work has shown a novel application of A*-based path planning for a multi-vehicle radio repeating operation. In this path planning, basic radio modeling techniques were used to serve as predictors for radio link health and when combining these techniques with the use of a well-informed and inflated heuristic, a unique path planner was created that could be rapidly executed to guide a ground vehicle to a goal location while maintaining strong radio repeating communication links between the various components of the operation. Additionally, not only have simulations shown the abilities of the path planner and its apparent superiority to the naïve radio repeating approaches discussed, but limited field testing has incorporated this path planner with a grander system architecture to perform the radio repeating operation on a vehicular system. This has both validated that the radio repeating operation is able to be executed on a vehicular system and has provided confidence that the path planner produces more favorable results than a potential naïve radio repeating variant. Therefore, this work presents not only a path planner, but the development of an entire system that may provide benefits to first responders and the robotics community alike.

References

[1]Mong-ying A. Hsieh, Vijay Kumar, and Camillo J. Taylor. "Constructing Radio Signal Strength Maps with Multiple Robots". In: *Proceedings of the 2004 IEEE International Conference on Robotics and Automation*. 2004.

[2]Charles W. Niessen. "Battlefield Connectivity via Airborne Communications Nodes". In: *Proceedings of the SPIE - The International Society for Optical Engineering*.

[3]Cory Dixon, Eric Frew, and Brian Argrow. "Radio Leashing of an Unmanned Aircraft". In: *Collection of Technical Papers - Infotech at Aerospace: Advancing Contemporary Aerospace Technologies and their Integration*. Vol. 2. 2005, pp. 1093-1102.

[4]Cory Dixon and Eric Frew. "Electronic Leashing of an Unmanned Aircraft to a Radio Source". In: *Proceedings of the 44th IEEE Conference on Decision and Control, and the European Control Conference*. 2005.

[5]Hoa G. Nguyen et al. "Autonomous Mobile Communication Relays". In: *Proceedings of the SPIE - The International Society for Optical Engineering*. 2002.

[6]H.G. Nguyen et al. "Autonomous Communication Relays for Tactical Robots". In: *Proceedings of ICAR 2003 - The 11th International Conference on Advanced Robotics*. 2003.

[7]Hoa G. Nguyen, Nathan Farrington, and Narek Pezeshkian. "Maintaining Communication Link for Tactical Ground Robots". In: *Proceedings of AUVSI's Unmanned Systems North America 2004*. 2004, pp. 311-323.

[8]Hoa G. Nguyen et al. "Maintaining Communication Link for a Robot Operating in a Hazardous Environment". In: *Proceedings of the 10th International Conference on Robotics and Remote Systems for Hazardous Environments*. 2004, pp. 256-263.

[9]L. Chaimowicz et al. "Deploying Air-Ground Multi-Robot Teams in Urban Environment". In: *Multi-Robot Systems- From Swarms to Intelligent Automata Volume III*. Ed. by Lynne Parker, Frank Schneider, and Alan Schultz. Springer Netherlands, 2005, pp. 223-234.

[10]Jonathan Fink and Vijay Kumar. "Online Methods for Radio Signal Mapping with Mobile Robots". In: *2010 IEEE International Conference on Robotics and Automation*. 2010.

[11]Mustafa Ayad, Peter Nielson, and R.M. Voyles. "RF Mapping for Intelligent Repeater Placement and Signal Recovery". In: *Emergency Management and Robotics for Hazardous Environments (EPRRSD)*. 2011.

[12]Steven M. LaValle. *Planning Algorithms*. Cambridge University Press, 2006.

[13]Dave Ferguson, Maxim Likhachev, and Anthony Stentz. "A Guide to Heuristic-based Path Planning". In: *Proceedings of ICAPS Workshop on Planning under Uncertainty for Autonomous Systems*. 2005.

[14]Eric A. Hansen and Rong Zhou. "Anytime Heuristic Search". In: *Journal of Artificial Intelligence Research* 28 (2007), pp. 267-297.

[15]Maxim Likhachev et al. "Anytime Search in Dynamic Graphs". In: *Artificial Intelligence Journal* 172.14 (2008), pp. 1613-1643.

[16]Bryan Krawiec et al. "Post Detonation Autonomous Robotic Response System". In: *Emergency Management and Robotics for Hazardous Environments (EPRRSD)*. 2011.

[17]Constantine A. Balanis. *Antenna Theory: Analysis and Design*. 3rd ed. Hoboken, NJ: John Wiley, 2005.

[18]Aleksandar Neskovic, Natasa Neskovic, and George Paunovic. "Modern Approaches in Modeling of Mobile Radio Systems Propagation Environment". In: *IEEE Communications Surveys* 3.3 (2000), pp. 2-12.

[19]Masaharu Hata. "Empirical Formula for Propagation Loss in Land Mobile Radio Services". In: *IEEE Transactions on Vehicular Technology* VT-29.3 (1980), pp. 317-325.

[20]Y. Okumura et al. "Field Strength and its Variability in VHF and UHF Land-Mobile Radio Service". In: *Review of the Electrical Communication Laboratory (Tokyo)* 16 (1968), pp. 825-873.

[21]Joram Walfisch and Henry L. Bertoni. "A Theoretical Model of UHF Propagation in Urban Environments". In: *IEEE Transactions on Antennas and Propagation* 36.12 (1988), pp. 1788-1796.

[22]V.S. Abhayawardhana et al. "Comparison of Empirical Propagation Path Loss Models for Fixed Wireless Access Systems". In: *IEEE Vehicular Technology Conference*. Vol. 61. 1. 2005, pp. 73-77.

[23]Nadia S. Adawi et al. "Coverage Prediction for Mobile Radio Systems Operating in the 800-900 MHz Frequency Range". In: *IEEE Transactions on Vehicular Technology* 37.1 (1988), pp. 3-72.

[24]John David Parsons. *The Mobile Radio Propagation Channel*. Chichester: John Wiley, 2000.